Cyano-Bridged Aqua(*N*,*N*-Dimethylacetamide)(cyanoiron)lanthanides from Samarium, Gadolinium, or Holmium Nitrate and Potassium Hexacyanoferrate: Crystal Structures and Magnetochemistry

by **Bing Yan**[a])[b]) and **Zhida Chen**[a])[b])*

[a]) State Key Laboratory of Rare Earth Material Chemistry and Applications, College of Chemistry and Molecular Engineering, Peking University, Beijing 100871, P.R. China

[b]) Peking University-Hong Kong University Joint Laboratory of Rare Earth Material and Bioinorganic Chemistry, Beijing 100871, P.R. China

Three cyano-bridged aqua(*N*,*N*-dimethylacetamide)(cyanoiron)lanthanide complexes were synthesized by the reaction of $K_3Fe(CN)_6$, $Ln(NO_3)_3 \cdot 6\,H_2O$ (Ln = Sm, Gd, Ho), and *N*,*N*-dimethylacetamide (DMA). The obtained complexes **1**–**3** exhibit different coordination geometries and crystal structures. The polymeric $\{[Sm(DMA)_2(H_2O)_4Fe(CN)_6 \cdot 5\,H_2O\}_n$ ($[SmFe]_n$; **1**) has a one-dimensional chain structure with approximately parallel *trans*-positioned bridging CN ligands between the Sm- and Fe-atoms. $[(Gd(DMA)_3(H_2O)_4)_2Fe(CN)_6] \cdot [Fe(CN)_6] \cdot 3\,H_2O$ (Gd_2Fe; **2**) is an isolated trinuclear Gd(1)–Fe–Gd(2) complex with two approximately perpendicular *cis*-positioned bridging CN ligands between the two Gd-atoms and the Fe-atom. $[Ho(DMA)_3(H_2O)_3Fe(CN)_6] \cdot 3\,H_2O$ (HoFe; **3**) adopts a single dinuclear crystal structure with only one bridging CN between the Ho- and Fe-atom. Magnetochemistry experiments establish weak antiferromagnetic interactions between Gd^{III} (and Ho^{III}) and Fe^{III} atoms. Especially the $[SmFe]_n$ complex **1** exhibits long-range magnetic ordering, $T_c = 3.5$ K, and a stronger coercive force, $H_c = 1400$ Oe.

Introduction. – Hexacyanometallate complexes have been widely studied in many fields, such as molecular-based magnets [1], in which particularly the Prussian blue analogues have shown fascinating magnetic properties with high T_c values [2] and magneto-optical phenomena [2b]. However, the spin-coupling mechanism between the metal ions in these Prussian blue analogues remains unknown due to a lack of crystal structures. For this purpose, crystal-structure analyses for a couple of cyano-bridged complexes have been performed, most of them being related to transition-metal ions [3]. It is worth pointing out that cyano-bridged lanthanide-transition metal complexes have rarely been reported, although rare-earth elements play an important role in magnetic materials. Furthermore, the magnetic 4f-3d molecular complexes synthesized so far mainly concern the Ln–Cu complexes [4]. In recent years, studies on (hexacyanometal) lanthanide complexes have been reported [5]. In the present work, we employed *N*,*N*-dimethylacetamide (DMA) as a hybrid ligand to synthesize three novel complexes: $\{[Sm(DMA)_2(H_2O)_4Fe(CN)_6] \cdot 5\,H_2O\}_n$ ($[SmFe]_n$; **1**), $[(Gd(DMA)_3(H_2O)_4)_2Fe(CN)_6] \cdot [Fe(CN)_6] \cdot 3\,H_2O$ (Gd_2Fe; **2**), and $[Ho(DMA)_3(H_2O)_3Fe(CN)_6] \cdot 3\,H_2O$ (HoFe; **3**). It is interesting that the complexes **1**–**3** exhibit three different coordination geometries and crystal structures, in spite of having the similar reactant and reaction conditions. The magnetic properties of **1**–**3**, especially of $[SmFe]_n$ complex **1**, were studied in detail.

Results and Discussion. – *Crystal Structures.* The crystal structure of $[SmFe]_n$ complex **1** (*Fig. 1* and *Table 1*) shows that the Sm-atom is eight-coordinate, bound by

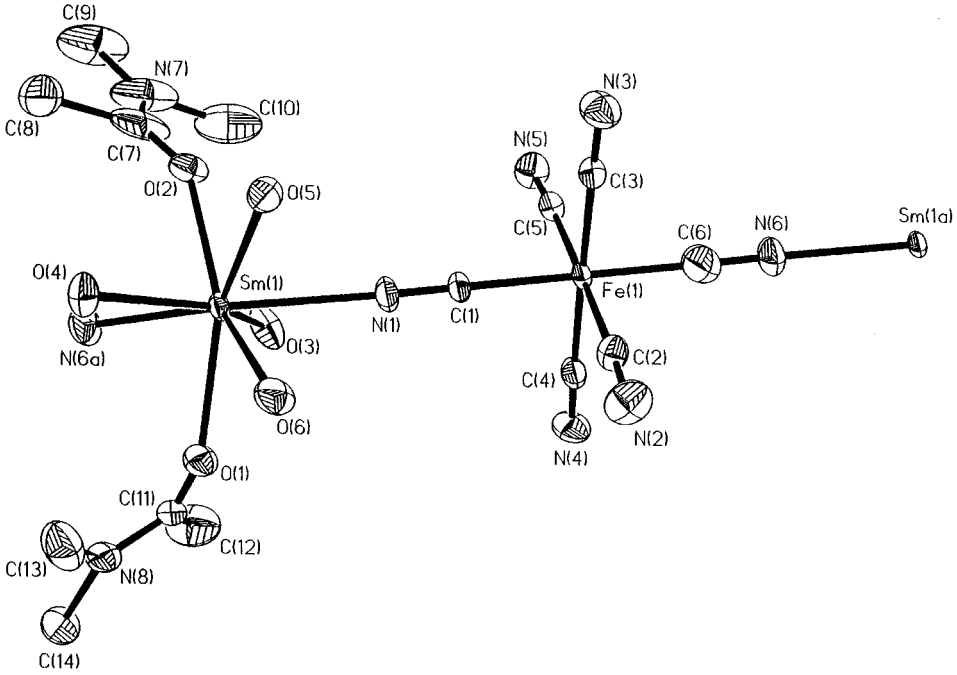

Fig. 1. *ORTEP Plot for the molecular structure of the complex [SmFe]*$_n$ (**1**)

Table 1. *Crystal Data and Structure Refinement for the Complexes [SmFe]*$_n$ (**1**), *Gd_2Fe* (**2**), *and HoFe* (**3**)

	1	**2**	**3**
Empirical formula	$C_{14}H_{36}FeN_8O_{11}Sm$	$C_{36}H_{76}Fe_2Gd_2N_{18}O_{17}$	$C_{18}H_{39}FeHoN_9O_9$
M_r	698.71	1459.35	746.36
Temperature [K]	293(2)	293(2)	293(2)
Wavelength [Å]	0.71073	0.71073	0.71073
Crystal system	monoclinic	orthorhombic	orthorhombic
Space group	$P2_1/n$	$P2_12_12$	$P2_12_12_1$
Unit-cell dimensions:			
a [Å]	10.2744(14)	18.969(4)	12.899(3)
b [Å]	16.732(2)	33.293(7)	12.975(3)
c [Å]	17.323(2)	9.556(2)	18.735(4)
β [°]	97.385(3)		
V [Å^3]	2953.3(7)	6035(2)	3135.6(12)
Z	4	4	4
Calc. density [Mg/m^3]	1.571	1.606	1.581
R_1	0.0412	0.0562	0.0589
wR_2	0.1072	0.1432	0.1430

six O-atoms of the two DMA molecules and four H_2O molecules as well as by two N-atoms from the two bridging CN ligands. The bond distances Sm–N are 2.528(5) (Sm–N(1)) and 2.549(5) Å (Sm–N(6)) (*Table 2*). The bond distances between Sm and the O-atoms of the H_2O molecules range from 2.404(5) to 2.550(5) Å, and those between Sm and the O-atoms of DMA are 2.321(4) and 2.329(4) Å. The bond angles of

Table 2. *Selected Bond Lengths* [Å] *of the Complexes [SmFe]*$_n$ (**1**), *Gd_2Fe* (**2**), *and HoFe* (**3**). For symmetry transformations used to generate equivalent atoms, see *Footnotes*.

Sm(1)–O(2)	2.321(4)	Sm(1)–N(6)[a])	2.549(5)	Fe(1)–C(6)	1.939(6)
Sm(1)–O(1)	2.329(4)	Sm(1)–N(1)	2.528(5)	N(6)–Sm(1)[b])	2.549(5)
Sm(1)–O(4)	2.404(5)	Sm(1)–O(6)	2.550(5)	N(1)–C(1)	1.136(7)
Sm(1)–O(3)	2.435(5)	C(1)–Fe(1)	1.947(6)	C(6)–N(6)	1.147(7)
Sm(1)–O(5)	2.467(4)				
Gd(1)–O(21)	2.303(11)	Gd(2)–O(41)	2.349(11)	Fe(2)–C(212)[c])	1.930(15)
Gd(1)–O(31)	2.314(10)	Gd(2)–O(5)	2.453(12)	Fe(2)–C(212)	1.930(15)
Gd(1)–O(11)	2.341(11)	Gd(2)–O(7)	2.463(11)	Fe(2)–C(213)[c])	1.955(17)
Gd(1)–O(4)	2.472(11)	Gd(2)–O(6)	2.481(10)	Fe(2)–C(213)	1.955(17)
Gd(1)–O(2)	2.492(11)	Gd(2)–O(8)	2.492(12)	Fe(3)–C(313)	1.924(15)
Gd(1)–O(1)	2.507(11)	Gd(2)–N(5)	2.543(15)	Fe(3)–C(313)[d])	1.924(15)
Gd(1)–O(3)	2.547(12)	Fe(1)–C(5)	1.892(14)	Fe(3)–C(312)[d])	1.938(16)
Gd(1)–N(6)	2.559(14)	Fe(1)–C(6)	1.921(16)	Fe(3)–C(312)	1.938(16)
Gd(2)–O(51)	2.316(11)	Fe(2)–C(211)	1.917(16)	Fe(3)–C(311)[d])	2.013(17)
Gd(2)–O(61)	2.338(11)	Fe(2)–C(211)[c])	1.927(16)	Fe(3)–C(311)	2.013(17)
Ho(1)–O(21)	2.204(18)	Ho(1)–O(2)	2.378(18)	Fe(1)–C(4)	1.94(3)
Ho(1)–O(31)	2.228(16)	Ho(1)–N(1)	2.415(18)	Fe(1)–C(1)	1.94(2)
Ho(1)–O(11)	2.230(15)	Fe(1)–C(3)	1.92(2)	Fe(1)–C(2)	1.95(2)
Ho(1)–O(3)	2.344(16)	Fe(1)–C(6)	1.937(18)	Fe(1)–C(5)	1.97(2)
Ho(1)–O(1)	2.359(17)				

[a]) For $[SmFe]_n$: $x-1/2$, $-y+3/2$, $z+1/2$. [b]) For $[SmFe]_n$: $x+1/2$, $-y+3/2$, $z-1/2$. [c]) For Gd_2Fe: $-x+2$, $-y+2$, z. [d]) For Gd_2Fe: $-x+1$, $-y$, z.

the bridging CN and Sm, *i.e.*, C(1)–N(1)–Sm and C(6)–N(6)–Sm, are 175.8(5) and 177.8(5)°, respectively, and that of N(1)–Sm–N(6) is 142.26(19)° (*Table 3*). The geometry of the $Fe(CN)_6^{3-}$ group is an approximate octahedron with the coordination of six CN ligands. The bond lengths Fe–C range from 1.933(7) to 1.953(7) Å, and the bond distances Fe–C(1) and Fe–C(6) implied in the bridging are 1.947(6) and 1.939(6) Å, respectively. The two bridging cyano ligands in **1** lead to a slight distortion of the bond angle C(1)–Fe(1)–C(6) (179.3(2)°). The bond angles Fe–C–N range from 176.9(6) to 178.7(6)°.

According to the unit-cell packing diagram of **1** (*Fig. 2*), two types of H-bonding are present. One is the intramolecular H-bond between the coordinated H_2O molecule in one complex unit and the CN of another complex unit. Another is the intermolecular H-bond involving an uncoordinated H_2O molecule present in the space within the unit cell of the complex. The O-atom of the uncoordinated H_2O molecule forms the H-bond with the coordinated H_2O molecule, while the uncoordinated H_2O molecule forms the other H-bond with the terminal CN group, thus representing an intermolecular H-bond tetrahedron. The H-bonds link the complex units and are responsible for the stability of the whole system. Because of the bond angle N(1)–Sm–N(6) of 142.26(19)° involving the two bridging CN of the one-dimensional chain –Fe–C(1)N(1)–Sm–N(6)C(6)–Fe–C(1)N(1)–Sm–, the structure **1** is similar to the β-folding chain of a protein molecule.

In the Gd_2Fe complex **2** (*Fig. 3*), the two Gd-atoms are each eight-coordinated, seven coordinating O-atoms belonging to the three DMA molecules and the four H_2O

Table 3. *Selected Bond Angles* [°] *for the Complexes [SmFe]*$_n$ (**1**), *Gd_2Fe* (**2**), *and HoFe* (**3**). For symmetry transformations used to generate equivalent atoms, see *Footnotes*.

N(6)[a]–Sm(1)–N(1)	142.26(19)	C(5)–Fe(1)–C(3)	92.5(3)	C(3)–Fe(1)–C(4)	178.6(2)
N(6)[a]–Sm(1)–O(6)	130.11(15)	C(6)–Fe(1)–C(3)	89.7(2)	C(1)–Fe(1)–C(4)	90.9(2)
N(1)–Sm(1)–O(6)	77.94(17)	C(2)–Fe(1)–C(1)	87.9(3)	N(2)–C(2)–Fe(1)	176.9(7)
C(1)–N(1)–Sm(1)	175.8(5)	C(5)–Fe(1)–C(1)	91.4(3)	N(3)–C(3)–Fe(1)	176.9(6)
N(1)–C(1)–Fe(1)	178.7(6)	C(6)–Fe(1)–C(1)	179.3(2)	N(4)–C(4)–Fe(1)	178.3(6)
C(2)–Fe(1)–C(5)	178.7(3)	C(3)–Fe(1)–C(1)	90.0(2)	N(5)–C(5)–Fe(1)	177.3(6)
C(2)–Fe(1)–C(6)	91.4(3)	C(2)–Fe(1)–C(4)	90.2(3)	N(6)–C(6)–Fe(1)	178.6(5)
C(5)–Fe(1)–C(6)	89.3(3)	C(5)–Fe(1)–C(4)	88.6(3)	C(6)–N(6)–Sm(1)[b]	177.8(5)
C(2)–Fe(1)–C(3)	88.7(3)	C(6)–Fe(1)–C(4)	89.4(2)		
O(31)–Gd(1)–N(6)	75.4(4)	C(4)–Fe(1)–C(1)	91.4(7)	C(312)[d]–Fe(3)–C(312)	91.1(9)
O(11)–Gd(1)–N(6)	73.2(5)	C(3)–Fe(1)–C(1)	90.0(7)	C(313)–Fe(3)–C(311)[d]	91.1(7)
O(4)–Gd(1)–N(6)	74.7(4)	C(2)–Fe(1)–C(1)	175.6(7)	C(313)[d]–Fe(3)–C(311)[d]	90.0(7)
O(2)–Gd(1)–N(6)	143.0(4)	O(21)–Gd(1)–N(6)	79.5(4)	C(312)[d]–Fe(3)–C(311)[d]	91.2(7)
O(1)–Gd(1)–N(6)	130.2(4)	C(211)–Fe(2)–C(211)[c]	87.7(10)	C(312)–Fe(3)–C(311)[d]	87.7(7)
O(3)–Gd(1)–N(6)	139.1(4)	C(211)–Fe(2)–C(212)[c]	92.1(7)	C(313)–Fe(3)–C(311)	90.0(7)
O(51)–Gd(2)–N(5)	138.2(5)	C(211)[c]–Fe(2)–C(212)[c]	88.3(6)	C(313)[d]–Fe(3)–C(311)	91.1(7)
O(61)–Gd(2)–N(5)	73.4(4)	C(211)–Fe(2)–C(212)	88.3(6)	C(312)[d]–Fe(3)–C(311)	87.7(7)
O(41)–Gd(2)–N(5)	73.1(4)	C(211)[c]–Fe(2)–C(212)	92.1(6)	C(312)–Fe(3)–C(311)	91.2(7)
O(5)–Gd(2)–N(5)	138.1(5)	C(212)[c]–Fe(2)–C(212)	79.4(9)	C(311)[d]–Fe(3)–C(311)	178.5(10)
O(7)–Gd(2)–N(5)	72.5(4)	C(211)–Fe(2)–C(213)[c]	77.3(7)	N(1)–C(1)–Fe(1)	177.9(16)
O(6)–Gd(2)–N(5)	134.7(5)	C(211)[c]–Fe(2)–C(213)[c]	90.6(7)	N(2)–C(2)–Fe(1)	177.1(13)
O(8)–Gd(2)–N(5)	67.9(5)	C(212)[c]–Fe(2)–C(213)	89.9(6)	N(3)–C(3)–Fe(1)	174.0(15)
C(6)–Fe(1)–C(5)	89.1(6)	C(212)–Fe(2)–C(213)[c]	89.7(7)	N(4)–C(4)–Fe(1)	179.0(14)
C(6)–Fe(1)–C(4)	90.7(7)	C(211)–Fe(2)–C(213)	90.6(7)	N(5)–C(5)–Fe(1)	176.3(13)
C(5)–Fe(1)–C(4)	178.7(6)	C(211)[c]–Fe(2)–C(213)	177.3(7)	N(6)–C(6)–Fe(1)	175.4(14)
C(6)–Fe(1)–C(3)	178.4(7)	C(212)[c]–Fe(2)–C(213)	89.7(7)	C(5)–N(5)–Gd(2)	176.8(13)
C(5)–Fe(1)–C(3)	92.6(6)	C(212)–Fe(2)–C(213)	89.9(6)	C(6)–N(6)–Gd(1)	163.1(13)
C(4)–Fe(1)–C(3)	87.7(7)	C(213)[c]–Fe(2)–C(213)	91.3(10)	N(211)–C(211)–Fe(2)	178.1(15)
C(6)–Fe(1)–C(2)	93.9(7)	C(313)–Fe(3)–C(313)[d]	88.1(9)	N(212)–C(212)–Fe(2)	175.9(14)
C(5)–Fe(1)–C(2)	90.4(6)	C(313)–Fe(3)–C(312)[d]	177.3(7)	N(213)–C(213)–Fe(2)	178.1(15)
C(4)–Fe(1)–C(2)	90.9(7)	C(313)[d]–Fe(3)–C(312)[d]	90.5(6)	N(311)–C(311)–Fe(3)	178.7(16)
C(3)–Fe(1)–C(2)	86.3(7)	C(313)–Fe(3)–C(312)	90.5(6)	N(312)–C(312)–Fe(3)	178.0(17)
C(6)–Fe(1)–C(1)	89.9(6)	C(313)[d]–Fe(3)–C(312)	177.3(7)	N(313)–C(313)–Fe(3)	174.8(16)
C(5)–Fe(1)–C(1)	87.3(6)				
O(21)–Ho(1)–N(1)	90.3(8)	C(6)–Fe(1)–C(1)	173.6(10)	C(1)–Fe(1)–C(5)	91.4(9)
O(31)–Ho(1)–N(1)	92.5(7)	C(4)–Fe(1)–C(1)	87.9(10)	C(2)–Fe(1)–C(5)	178.2(10)
O(11)–Ho(1)–N(1)	179.6(7)	C(3)–Fe(1)–C(2)	87.4(10)	N(1)–C(1)–Fe(1)	178.3(18)
O(3)–Ho(1)–N(1)	90.9(6)	C(6)–Fe(1)–C(2)	91.0(10)	C(1)–N(1)–Ho(1)	162.9(18)
O(1)–Ho(1)–N(1)	83.3(6)	C(4)–Fe(1)–C(2)	91.7(12)	N(2)–C(2)–Fe(1)	176(3)
O(2)–Ho(1)–N(1)	88.6(7)	C(1)–Fe(1)–C(2)	88.6(10)	N(3)–C(3)–Fe(1)	175(2)
C(3)–Fe(1)–C(6)	91.1(9)	C(3)–Fe(1)–C(5)	90.9(10)	N(4)–C(4)–Fe(1)	175(3)
C(3)–Fe(1)–C(4)	176.8(10)	C(6)–Fe(1)–C(5)	89.2(10)	N(5)–C(5)–Fe(1)	173(2)
C(6)–Fe(1)–C(4)	85.8(9)	C(4)–Fe(1)–C(5)	90.1(10)	N(6)–C(6)–Fe(1)	177(2)
C(3)–Fe(1)–C(1)	95.2(10)				

[a]) For $[SmFe]_n$: $x-1/2$, $-y+3/2$, $z+1/2$. [b]) For $[SmFe]_n$: $x+1/2$, $-y+3/2$, $z-1/2$. [c]) For Gd_2Fe: $-x+2$, $-y+2$, z. [d]) For Gd_2Fe: $-x+1$, $-y$, z.

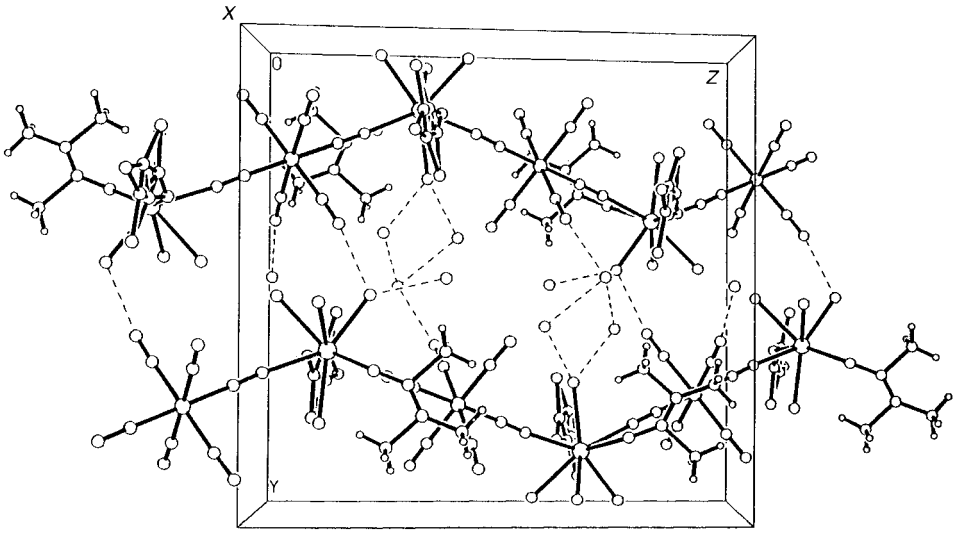

Fig. 2. *Unit-cell packing diagram of the complex* $[SmFe]_n$ (**1**)

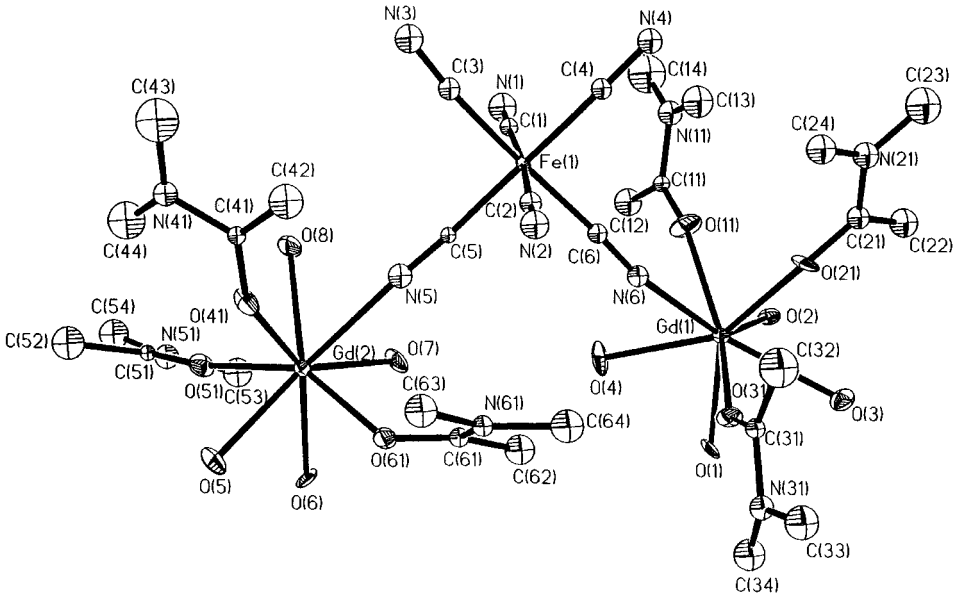

Fig. 3. *ORTEP Plot for the molecular structure of the complex* Gd_2Fe (**2**)

molecules, and one coordinating N-atom belonging to the bridging CN ligand. The Fe-atom is connected to two Gd-atoms *via* two bridging CN groups (C(5)N(5) and C(6)N(6)). It is interesting that one DMA molecule coordinated to the Gd-atom adopts two different stereo configurations, in which the only difference is that all atoms of this DMA ligand are rotated by 180° around the O–Gd axis, except the coordinated

O-atom. *Fig. 3* shows only one configuration. The two stereo configurations in the unit-cell model are responsible for some disorder in the structure of complex **2**. The distances Gd–N are 2.559(14) (Gd(1)–N(6)) and 2.543(15) Å (Gd(2)–N(5)), respectively (*Table 2*). The distances between Gd(1) and Gd(2) and the O-atoms of the coordinated H_2O are in the range 2.472(11) – 2.547(12) and 2.453(13) – 2.492(12) Å, respectively. The distances between Gd(1) and Gd(2) and the O-atoms of the coordinated DMA molecules are 2.303(11) – 2.341(11) and 2.316(11) – 2.349(11) Å, respectively. The bond angles between the bridging CN and Gd(1) and Gd(2) (C–N–Gd) amount to 163.1(13) and 176.8(13)°, respectively (*Table 3*). The Fe-atom of **2** has six coordinated CN groups and adopts a distorted octahedral conformation. The crystal structure of **2** indicates that there is a central cyano-bridged framework. The bond lengths Fe–C range from 1.892(14) to 1.947(15) Å, Fe(1)–C(5) and Fe(1)–C(6) involved in the bridging CN being 1.892(14) and 1.921(16) Å, respectively. The bond angles C–Fe–C are typical of the distortion of the octahedron, due to the two bridging CN, and the bond angle C(5)–Fe(1)–C(6) is 89.1(6)°. The bond angles Fe–C–N range from 174.0(14) and 179.0(14)°.

In the space of the unit cell of complex **2**, there are three uncoordinated H_2O molecules and a counterion $[Fe(CN)_6]^{3-}$ that form H-bonds with the complex moiety, thus stabilizing the whole system. The uncoordinated H_2O molecules also form the intramolecular H-bonds with the coordinated H_2O molecules as well as with the N-atom of the CN ligand within the same unit, thus creating a network structure. In the trinuclear structure Gd(1)–N(6)C(6)–Fe–C(5)N(5)–Gd(2) of **2**, the two *cis*-located CN groups bridge one Fe-atom and two Gd-atoms, generating an isolated molecular structure that differs from the chain-like structure in the $[SmFe]_n$ complex **1** generated by the *trans*-located bridging CN ligands.

The HoFe complex **3** has a neutral CN-bridged dinuclear structure (*Fig. 4*). The Ho-atom is seven-coordinate, and the coordination polyhedron can be described as a slightly distorted pentagonal bipyramid. The six O-atoms of three H_2O molecules and three DMA molecules and one N-atom of the bridging CN ligand coordinate to the Ho-atom with the Ho–O distance ranging from 2.204(18) to 2.378(18) Å. The geometry of the $Fe(CN)_6^{3-}$ moiety is approximately octahedral, the Fe–C distances being 1.92(2) – 1.97(2) Å. The C≡N bond lengths vary from 1.10(3) to 1.18(3) Å, and the Fe–C≡N bond angles do not significantly deviate from linearity. However, the bridging CN ligand coordinates to the Ho-atom in a bent mode, which may be due to the effect of steric hindrance by the coordinated DMA molecules around the Ho-atom. Three uncoordinated H_2O molecues, represented by O(4), O(5), and O(6), are H-bonded to the coordinated H_2O molecules (O(1), O(2), and O(3)) with the contacts O(1)···O(4) of 2.732 Å, O(1)···O(5) of 2.693 Å, and O(2)···O(4) of 2.686 Å. In addition, the terminal CN ligands are also H-bonded to some H_2O molecules of the adjacent Ho–Fe fragment.

The crystal structures of the three complexes **1** – **3** clearly establish that there exists a great variety of structures that can be adopted by the different lanthanide ions (light rare earth Sm → central rare earth Gd → heavy rare earth Ho). This is of uppermost importance and interest for the study of rare-earth coordination chemistry and structural chemistry.

Magnetochemistry. The variable-temperature susceptibilities for the complexes **1** – **3** (1.8 – 300 K) were measured by a *MagLab-2000* magnetometer under the applied

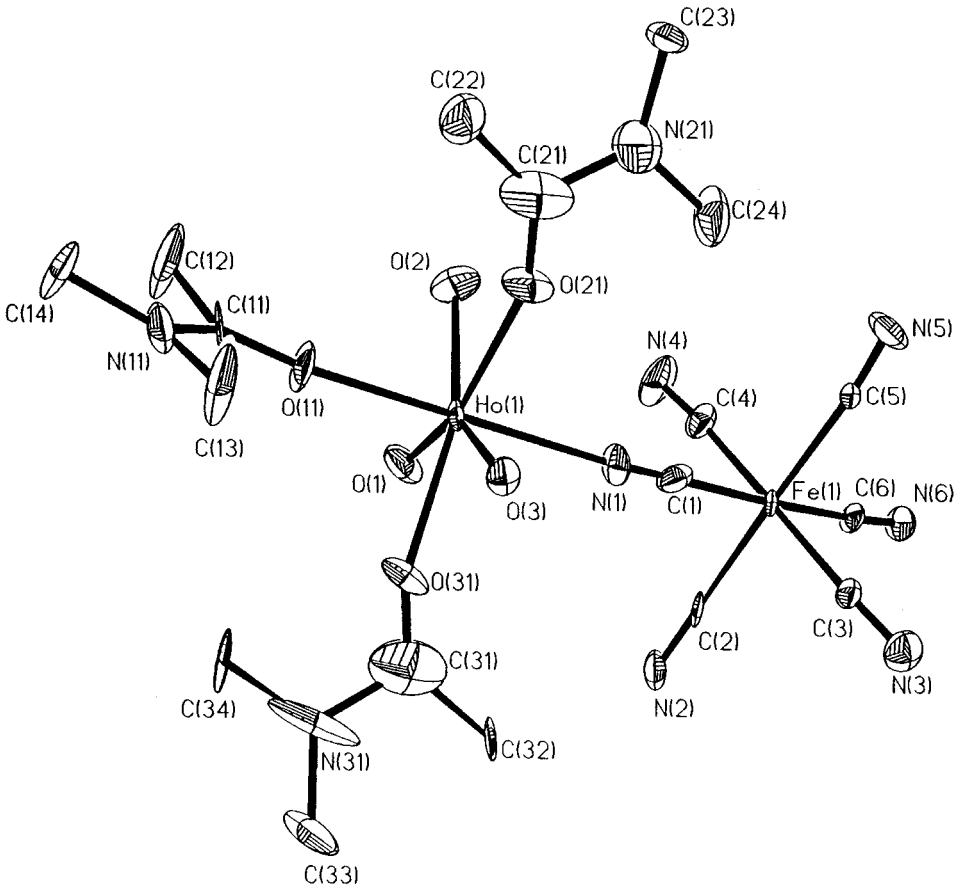

Fig. 4. *ORTEP Plot for the molecular structure of the complex HoFe* (**3**)

magnetic field of 10000 Oe. *Fig. 5* shows the plot of $\chi_m^{-1} - T$ and $\chi_m T - T$ for the HoFe complex **3**. The χ_m^{-1} *vs.* T in the variable-temperature susceptibility curve for **3** is nearly a straight line in the higher temperature range, which obeys the *Curie-Weiss* law. The *Curie* and *Weiss* constants, C and θ, are 16.56 cm^3 K mol^{-1} and -2.22 K for HoFe, respectively, based on the equation $\chi_m = C/(T-\theta)$. Similar results can be obtained for the Gd_2Fe complex **2**, the *Curie* and *Weiss* constant, C and θ, being 2.26 cm^3 K mol^{-1} and -44.3 K, respectively. The negative *Weiss* constants indicate an overall intramolecular antiferromagnetic interaction between the adjacent Gd^{III} ($S = 7/2$), Ho^{III} ($S = 2$), and Fe^{III} ($S = 1/2$) ions through the CN bridge. For the $[SmFe]_n$ complex **1**, the $\chi_m T$ decreases from 1.632 cm^3 K mol^{-1} at 300 K to 0.533 cm^3 K mol^{-1} at 8.85 K, then sharply increases below 8.85 K, which suggests the occurrence of a weak ferrimagnetic phase transition.

We further measured the magnetic susceptibility for the crystal sample of the $[SmFe]_n$ complex **1** in the lower temperature range (1.8–9 K) under an applied magnetic field of 1000 Oe (*Fig. 6*). The results suggest a weak ferrimagnetic behavior

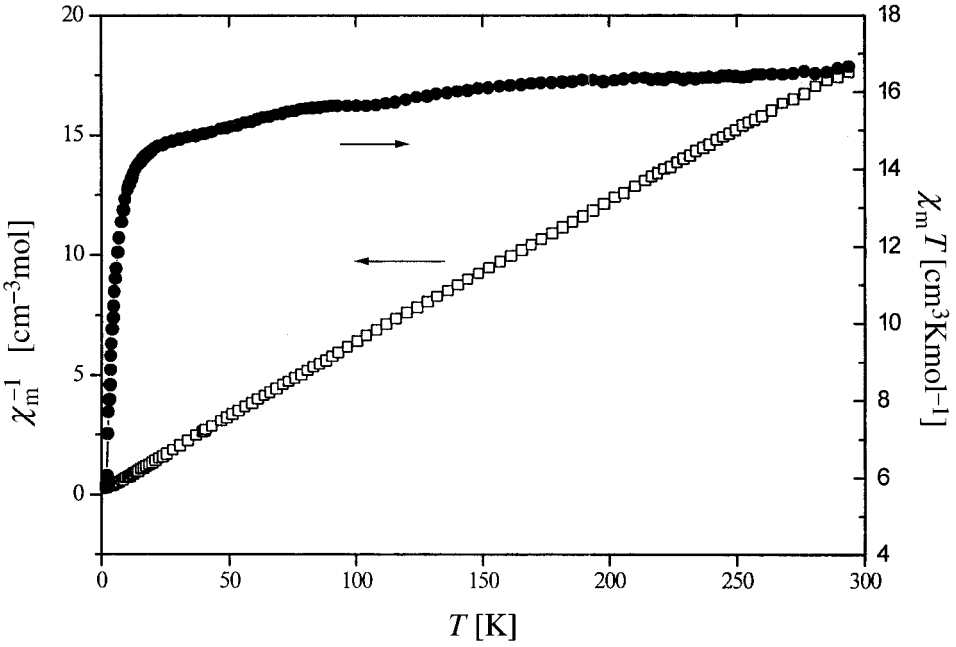

Fig. 5. *Variable-temperature* (1.8–300 K) *susceptibility of the complex HoFe* (**3**)

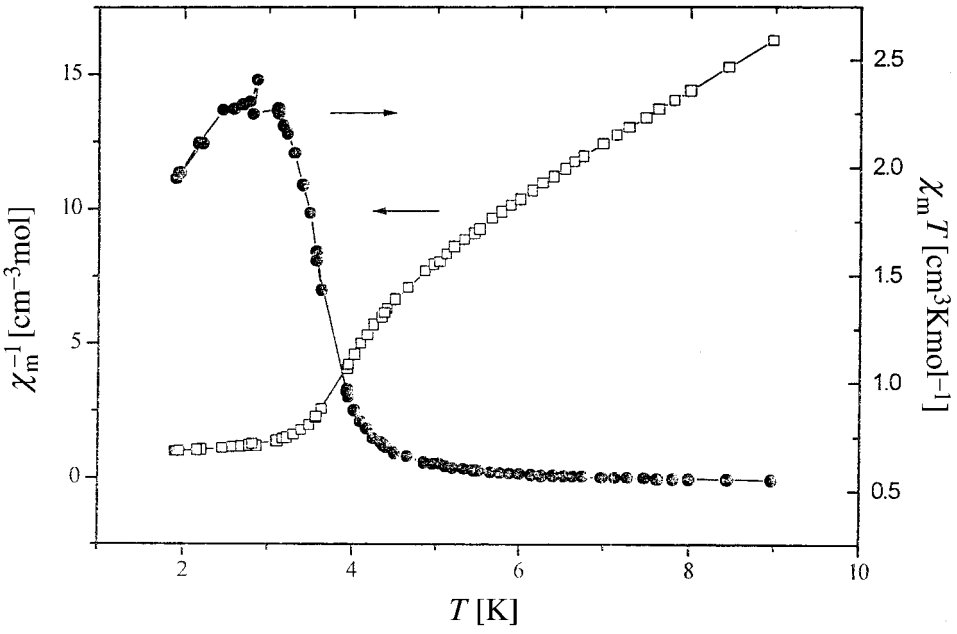

Fig. 6. *Variable low-temperature* (1.8–9 K) *susceptibility of the complex* $[SmFe]_n$ (**1**)

of **1** between 1.8 and 6 K. The $\chi_m T$ value is 0.58 cm^3 K mol^{-1} at 6 K and then increases sharply up to a maximum value of 2.30 cm^3 K mol^{-1} at 3.0 K and then decreases quickly below this temperature. The weak ferrimagnetic behavior of the one-dimensional structure of **1** suggests the onset of three-dimensional magnetic ordering. The decrease of $\chi_m T$ below 3 K results from an intermolecular antiferromagnetic coupling.

In *Fig. 7*, the temperature dependence of the alternate-current (AC) magnetic susceptibility shows that both in-phase, χ', and out-of-phase, χ'', components of the AC magnetic susceptibility exist for **1** in the temperature range 2.2 – 5.5 K. The measurements were made by cooling the compound in a close to zero field and then measuring at a driving frequency of 199 (*Fig. 7,a*) and 355 Hz (*Fig. 7,b*) with zero-applied DC field. The observation of χ'' is due to a long-range magnetic ordering in certain extent, and consequently, a strong coercive behavior is expected. When the external magnetic field is reversed with a certain frequency in the AC susceptibility experiment, the magnetization of the sample must respond to this oscillating external magnetic field. In the case of a simple paramagnet, the magnetization of the sample can relax very rapidly (nanoseconds), and can follow the oscillating external field. Thus, no out-of-phase component (imaginary part) of the AC susceptibility is expected for the simple paramagnet. If the magnetization of the sample relaxes slowly, then there must be a nonzero imaginary component. The $[SmFe]_n$ complex **1** exhibits one temperature dependent χ'' peak in the region 2.2 – 4.0 K. This is consistent with the χ' *vs.* temperature plots, where there is also a peak in the range 2.2 – 4.0 K. The T_c is best determined to be 3.5 K by the first $\chi'(T)$ peak maximum.

Fig. 8 gives the field-dependent magnetization (*M vs. H*) hysteresis data for the $[SmFe]_n$ complex **1** under the applied magnetic field from -2000 to $+2000$ Oe at 1.8 K. It is interesting to note that this hysteresis loop reveals a stronger coercive field H_c of 1400 Oe and a remnant magnetization M_R of 0.11 Nβ mol^{-1}. It is worth pointing out that thus the one-dimensional chain structure of $[SmFe]_n$ complex **1** exhibits the magnetic properties of a three-dimensional system. Nevertheless, this strange magnetic behavior is ascribed to the stronger interaction between different chains of the complex.

In conclusion, under the same reaction conditions and with similar reactants, three novel cyano-bridged complexes with quite different crystal structures were obtained. The $[SmFe]_n$ complex **1** has a one-dimensional chain structure with *trans*-positioned CN bridges between the Fe- and Sm-atom, while Gd_2Fe complex **2** forms an isolated trinuclear structure due to two *cis*-located CN bridges between one Fe- and two Gd-atoms. The HoFe complex **3** adopts a simple dinuclear structure. Especially **1** exhibits excellent magnetic properties, with the observation of an out-of-phase component of the alternate-current magnetic susceptibility showing the long-range magnetic order and the hysteresis loop typical for a strong coercive behavior. To the best of our knowledge, this complex is the first example of an X-ray-analyzed one-dimensional cyano-bridged rare earth/iron structure magnet with long-range magnetic ordering, higher T_c, and stronger coercive force.

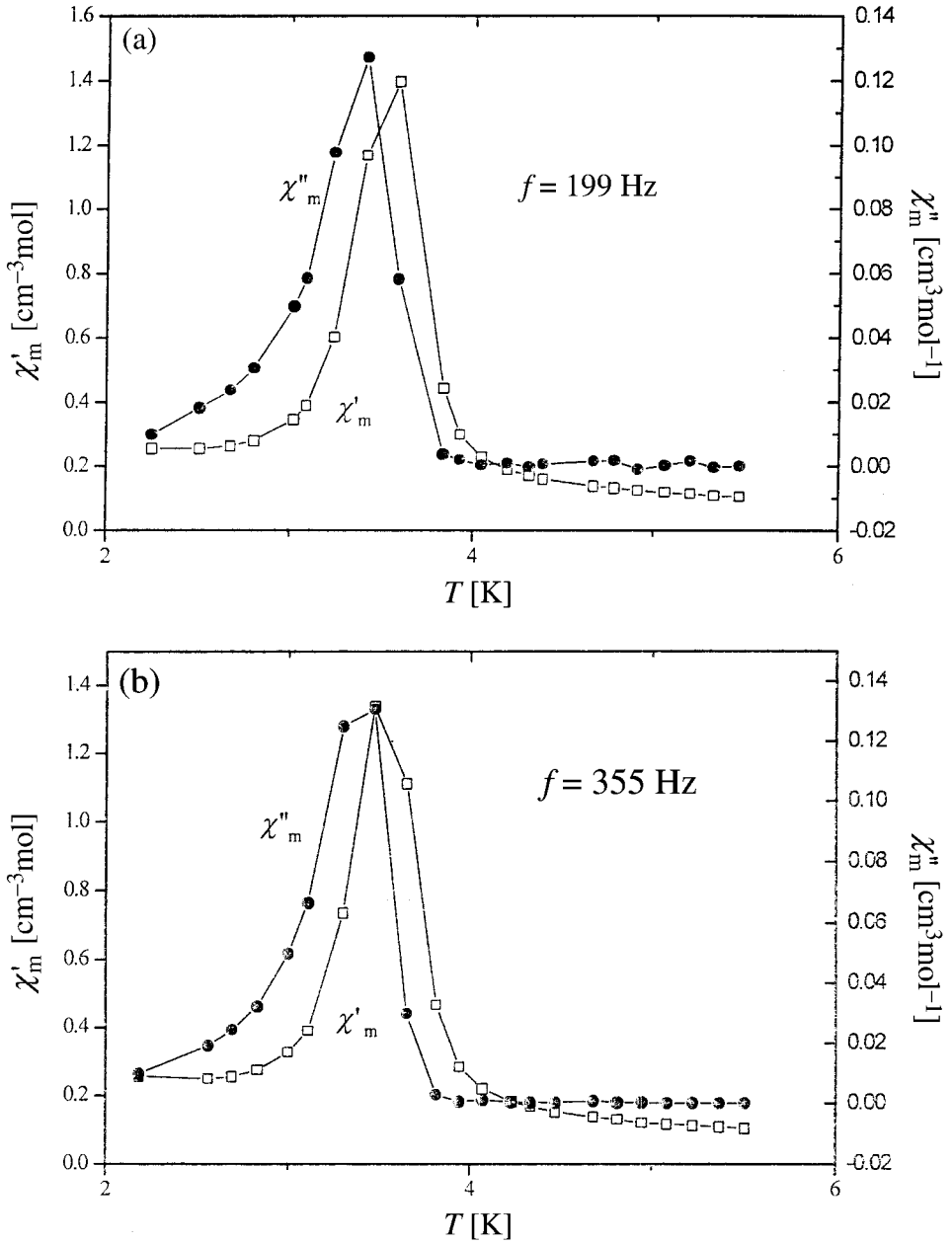

Fig. 7. *Plot of the in-phase and out-of-phase alternating-current magnetic susceptibility for the complex* $[SmFe]_n$ (**1**) *at driving frequency of* a) *199 Hz and* b) *355 Hz*

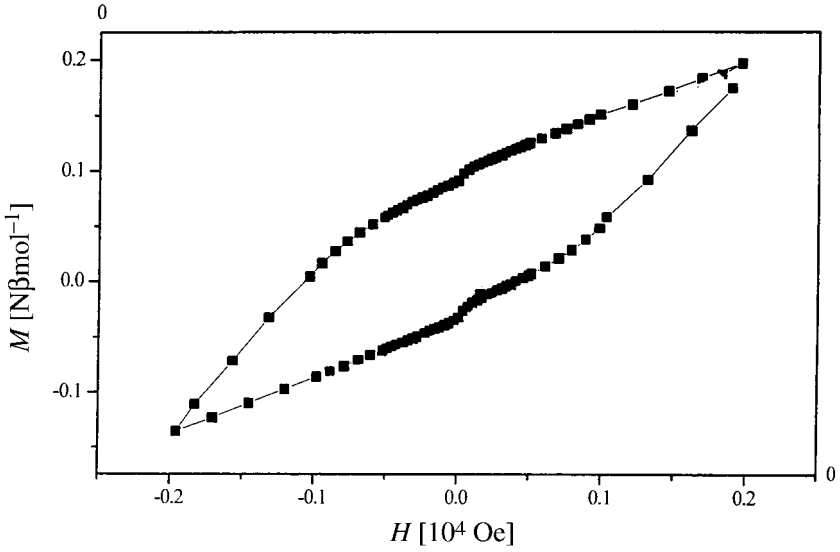

Fig. 8. *Hysteresis loop of the complex [SmFe]*$_n$ (**1**) *at 1.8 K*

Experimental Part

General. $K_3[Fe(CN)_6]$, lanthanide(III) nitrate, and *N,N*-dimethylacetamide (DMA) were purchased from *Aldrich* and used without purification. IR Spectra: KBr pellets; *Nicolet 7199B* spectrophotometer, 4000–400 cm^{-1} region; $\tilde{\nu}$ in cm^{-1}. Variable-temperature magnetic susceptibilities (1.8–300 K): *MagLab 2000* magnetometer; data corrected for diamagnetism of all the constituent atoms with *Pascal*'s constants. Elemental analyses (C, H, N): *Elementar Cario EL* elemental analyzer.

Synthesis of the Complexes. To a DMA soln. of $Ln(NO_3)_3 \cdot 6\,H_2O$ ($Sm(NO_3)_3 \cdot 6\,H_2O$, 0.444 g; $Gd(NO_3)_3 \cdot 6\,H_2O$, 0.453 g; $Ho(NO_3)_3 \cdot 6\,H_2O$, 0.461; 1.0 mmol), $K_3[Fe(CN)_6]$ (1.0 mmol) dissolved in a minimum amount of H_2O was added slowly. The transparent yellow soln. was filtered and kept in the dark to prevent hydrolysis of $K_3[Fe(CN)_6]$. After about one month, orange-yellow crystals were obtained.

Data of **1**: IR (main bands): 3422 (OH); 2119, 2141 (C–N), 1654, 1673 (C–O, DMA). Anal. calc. for $C_{14}H_{36}FeN_8O_{11}Sm$: C 24.05, H 5.16, N 16.09; found: C 24.47, H 5.02, N 15.93.

Data of **2**: IR (main bands): 3417 (OH), 2120, 2142 (C–N), 1654, 1673 (C–O, DMA). Anal. calc. for $C_{36}H_{76}Fe_2Gd_2N_{18}O_{17}$: C 29.60, H 5.21, N 17.27; found: C 29.39, H 5.07, N 17.77.

Data of **3**: IR (main bands): 3415 (H–O), 2122, 2140 (C–N), 1652, 1672 (C–O, DMA). Anal. calc. for $[Ho(DMA)_3(H_2O)_3Fe(CN)_6] \cdot 3\,H_2O$: C 28.94, H 5.23, N 16.88; found: C 28.74, H 5.07, N 17.91.

Crystal Data Collection and Refinement (*Table 1*). *Tetraaqua[μ-(cyano-*κ*C:*κ*N)]bis(N,N-dimethylacetamide-*κ*O)[pentakis(cyano-*κ*C)iron]samarium Hydrate (1:5) Homopolymer* (**1**; $\{[(Sm(DMA)_2(H_2O)_4Fe(CN)_6] \cdot 5\,H_2O\}_n$; $[SmFe]_n$)[1]. A red crystal of **1** (0.30 × 0.25 × 0.20 mm) was mounted on a *CCD* area detector operating with graphite-monochromated MoK_α radiation (λ 0.71073 Å). In total, 10284 reflection intensity data were collected, of which 5124 independent reflections were measured in the range $2.19 \leq \theta < 25.02°$ at 273(2) K by the ω-2θ scan mode. An empirical absorption correction was applied by means of the SADABS, which gave the transmission factors: min/max 0.52/0.87. The crystal structure was solved by direct methods and *Fourier* synthesis with the program SHELXS-97 and refined by the full-matrix least-squares method on F^2, with the program SHELXL-97. The function minimized was $\Sigma w(|F_o|^2 - |F_c|^2)^2$ where $w = [s^2(F_o^2) + (0.0727P)^2 +$

[1]) Crystallographic data for the structures reported in this paper have been deposited with the *Cambridge Crystallographic Data Center* as supplementary publication no. CCDC-144102, 144103, and 146353. Copies of the data can be obtained, free of charge, on application to the director, CCDC, 12 Union Road, Cambridge CB2 1EZ, UK (fax: (+44) (1223) 336-033; e-mail: deposit@ccdc.cam.ac.uk).

$0.0000P]^{-1}$ and $P = (F_o^2 + 2\,F_c^2)/3$. Primary non-H-atoms were solved by the directly method and secondary non-H-atoms were solved by difference maps. The H-atoms were added geometrically and refined by mixed methods. Some disorders were observed for **1**. In all, 334 parameters were refined for 5124 reflections. An approximate (isotropic) treatment of cell ellipsoids was used for estimating ellipsoids involving left-side planes. Refinement converged at R (on F) 0.0412, wR (on F^2) 0.1072. Maximum and minimum peaks in the final difference maps were 1.252 e · Å^{-3} and −1.312 e · Å^{-3}, respectively.

*Octaaquabis[*μ*-(cyano-*κ*C:*κ*N)]hexakis(*N,N*-dimethylacetamide-*κ*O)[tetrakis(cyano-*κ*C)iron]digadolinium Hexakis(cyano-*κ*C)ferrate(3 −) Hydrate (1:1:3)*; **2** [$(Gd(DMA)_3(H_2O)_4)_2Fe(CN)_6]\cdot 3\,H_2O$; Gd_2Fe)[1]). A red crystal (0.30 × 0.30 × 0.25 mm) was selected and mounted on an *Enraf-Nonius* four-circle *CAD-4* diffractometer. Intensities were collected with graphite-monochromated MoK_α radiation (λ 0.71073 Å) by the ω-2θ scan mode. In all, 5724 reflection intensity data were collected, of which 5724 independent reflections were measured in the range $2.13 \leq \theta \leq 25.03°$ at 273(2) K. An empirical absorption correction was applied by means of the DIFABS, which gave the transmission factors: min/max 0.893/1.109 2.19. The crystal structure was solved by direct methods, with the program SHELXS-97 as described for **1**. Some disorders were observed for **2**. In all, 440 parameters were refined for 5724 reflections. Refinement converged at R (on F) 0.0562, wR (on F^2) 0.1432. Maximum and minimum peaks in the final difference maps were 1.425 e · Å^{-3} and −1.240 e · Å^{-3}, respectively.

*Triaqua[*μ*-(cyano-*κ*C:*κ*N)]tris(N,N-dimethylacetamide-*κ*O)[pentakis(cyano-*κ*C)iron]holmium Hydrate (1:3)* (**3**; $[Ho(DMA)_3(H_2O)_3Fe(CN)_6]\cdot 3\,H_2O$; HoFe)[1]). A light-yellow crystal (0.50 × 0.30 × 0.20 mm) was selected and mounted on an *Enraf-Nonius* four-circle *CAD-4* diffractometer. Intensities were collected with graphite-monochromated MoK_α radiation (λ 0.71073 Å) by the ω-2θ scan mode. In all, 2924 reflection intensity data were collected, of which 2934 independent reflections were measured in the range $2.17 \leq \theta \leq 24.96°$ at 273(2) K. An empirical absorption correction was applied by means the Psi scan, which gave the transmission factors: min/max 0.479/0.9970. The crystal structure was solved by direct methods with the program SHELXS-97 as described for **1**. Some disorders were observed for **3**, which showed some anisotropic ellipsoids. In all, 343 parameters were refined for 2934 reflections. Refinement converged at R (on F) 0.0589, wR (on F^2) 0.1430. Maximum and minimum peaks in the final difference maps were 2.452 e · Å^{-3} and −2.266 e · Å^{-3}, respectively.

This work was supported by the *National Natural Science Foundation of China* (29831010, 20023005), the *State Key Project of Fundamental Research of China* (G1998061306), and the *China Postdoctoral Science Foundation.*

REFERENCES

[1] 'Molecular Magnetic Materials', Eds. D. Gatteschi, O. Kahn, J. S. Miller, and F. Palacio, Kluwer Academic, Dordrecht, The Netherlands, 1991, p. 198.

[2] a) V. Gadet, T. Mallah, I. Castro, M. Verdaguer, P. Veillet, *J. Am. Chem. Soc.* **1992**, *114*, 9213; b) T. Mallah, S. Thiebaut, M. Verdaguer, P. Veillet, *Science (Washington, D.C.)* **1993**, *262*, 1554; c) W. R. Entley, G. S. Girolami, *Science (Washington, D.C.)* **1995**, *268*, 397; O. Sato, T. Iyoda, A. Fujishima, K. Hashimoto, *Science (Washington, D.C.)* **1996**, *271*, 49; S. Ferlay, T. Mallah, R. Ouahes, P. Veillet, M. Verdaguer, *Nature (London)* **1995**, *378*, 701; O. Sato, T. Iyoda, A. Fujishima, K. Hashimoto, *Science (Washington, D.C.)* **1996**, *272*, 704.

[3] D. G. Fu, J. Chen, X. S. Tan, J. J. Li, S. W. Zhang, P. J. Zheng, W. X. Tang, *Inorg. Chem.* **1997**, *36*, 220; M. Ohba, H. Okawa, N. Fukita, Y. Hashimoto, *J. Am. Chem. Soc.* **1997**, *119*, 1011; H. Miyasaka, N. R. N. Matsumoto, E. Gallo, C. Floriani, *Inorg. Chem.* **1997**, *36*, 670; M. Ohba, N. Fukita, H. Okawa, *J. Chem. Soc., Dalton Trans.* **1997**, 1733; S. Ferlay, T. Mallah, J. Vaissermann, F. Bartolome, P. Veillet, M. Verdaguer, *J. Chem. Soc., Chem. Commun.* **1996**, 2481; R. J. Parker, D. C. R. Hockless, B. Moubaraki, K. S. Murray, L. Spiccia, *J. Chem. Soc., Chem. Commun.* **1996**, 2789; H. Z. Kou, D. Z. Liao, P. Cheng, Z. H. Jiang, S. P. Yan, G. L. Wang, X. K. Yao, H. G. Wang, *J. Chem. Soc., Dalton Trans.* **1997**, 1503.

[4] L. Q. Chen, S. R. Breeze, R. J. Rousseau, S. N. Wang, L. K. Thompson, *Inorg. Chem.* **1995**, *34*, 454; O. Kahn, O. Guillou, R. L. Oushoorn, M. Drillon, P. Rabu, K. Boubekeur, P. Batail, *New J. Chem.* **1995**, *19*, 655; X. M. Chen, M. L. Tong, Y. L. Wu, Y. J. Luo, *J. Chem. Soc., Dalton Trans.* **1996**, 2181; X. M. Chen, Y. L. Wu, Y. Y. Yang, S. M. J. Aubin, D. N. Hendrickson, *Inorg. Chem.* **1998**, *37*, 6186; J. P. Costes, F. Dahan, A. Dupuis, J. P. Laurent, *Inorg. Chem.* **1996**, *35*, 2400; J. P. Costes, F. Dahan, A. Dupuis, J. P. Laurent, *Inorg. Chem.* **1997**, *36*, 3429; J. P. Costes, F. Dahan, A. Dupuis, *Inorg. Chem.* **2000**, *39*, 165; J. P. Costes, F. Dahan, A. Dupuis, J. P. Laurent, *Inorg. Chem.* **2000**, *39*, 169; J. L. Sanz, R. Ruiz, A. Gleizes, F. Lloret, J. Faus, M. Julve, J. J.

BorrasAlmenar, Y. Journaux, *Inorg. Chem*. **1996**, *35*, 7384; I. Ramade, O. Kahn, Y. Jeannin, F. Robert, *Inorg. Chem*. **1997**, *36*, 930.

[5] E. Traversa, P. Nunziante, M. Sakamoto, K. Watanabe, Y. Sadaoka, Y. Sakai, *Chem. Lett*. **1995**, 189; Y. Sadaoka, E. Traversa, M. Sakamoto, *Chem. Lett*. **1996**, 177; D. W. Knoeppel, S. G. Shore, *Inorg. Chem*. **1996**, *35*, 1747; H. B. Deng, S. H. Chun, D. Florian, P. J. Grandinetti, S. G. Shore, *Inorg. Chem*. **1996**, *35*, 3891; D. W. Knoeppel, S. G. Shore, *Inorg. Chem*. **1996**, *35*, 5328; J. P. Liu, E. A. Meyers, J. A. Cowan, S. G. Shore, *Chem. Commun.* **1998**, 2043; D. W. Knoeppel, J. P. Liu, E. A. Meyers, S. G. Shore, *Inorg. Chem*. **1998**, *37*, 4828; B. Du, E. A. Meyers, S. G. Shore, *Inorg. Chem*. **2000**, *39*, 4639; D. F. Mullica, P. K. Hayward, E. L. Sappenfield, *Inorg. Chim. Acta* **1996**, *244*, 273; Z. Assefa, G. Shankle, H. H. Patterson, R. Reynolds, *Inorg. Chem*. **1994**, *33*, 2187; Z. Assefa, H. H. Patterson, *Inorg. Chem*. **1994**, *33*, 6194; H. Z. Kou, G. M. Yang, D. Z. Liao, P. Cheng, Z. H. Jiang, S. P. Yan, X. Y. Huang, G. L. Wang, *J. Chem. Crystallogr.* **1998**, *28*, 1503; S. Gao, B. Q. Ma, Z. M. Wang, C. H. Yan, G. X. Xu, *Mol. Cryst. Liq. Cryst.* **1999**, *335*, 201; B. Yan, H. D. Wang, Z. D. Chen, *Inorg. Chem. Commun*. **2000**, *3*, 653.

Received October 16, 2000